

Newly-Developed 3D GRMHD Code and its Application to Jet Formation

Y. Mizuno (NSSTC/MSFC/NPP),

collaborator

K.-I. Nishikawa (NSSTC/UAH), P. Hardee (UA),

S. Koide (Kumamoto Univ.),

G.J. Fishman (NSSTC/MSFC)

NSSTC colloquium, Sep 8 2006

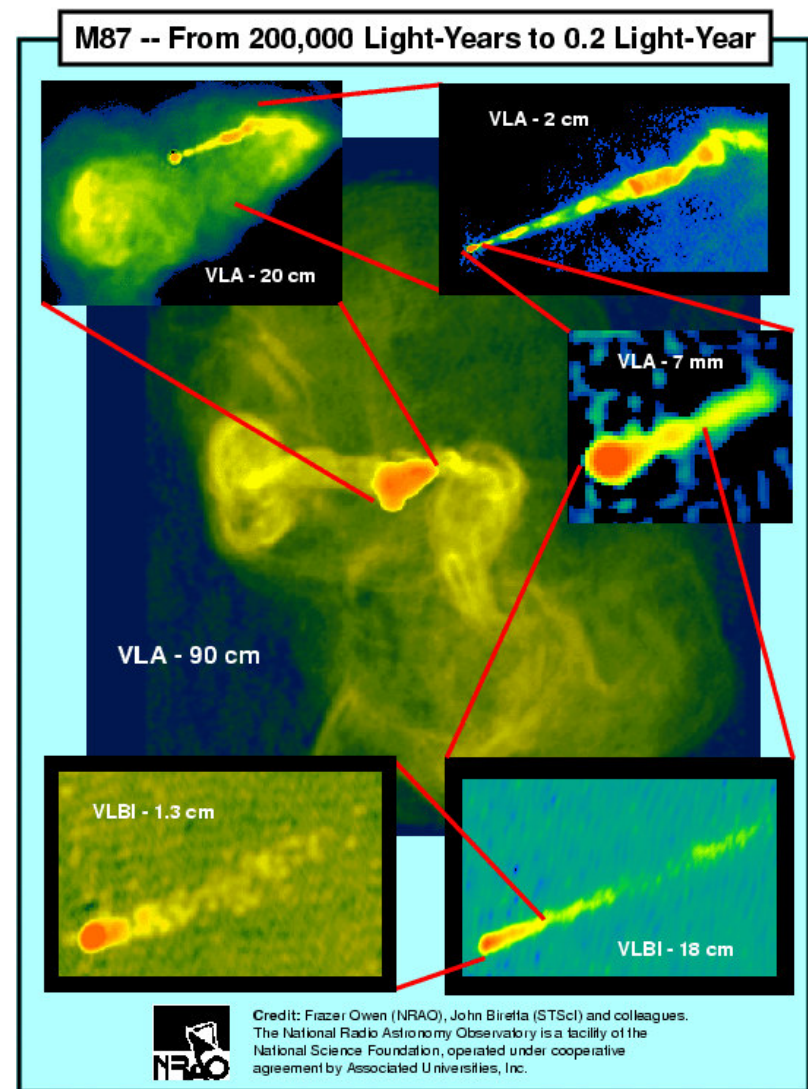
Introduction

- Magnetic and gravitational fields play a important role in determining the evolution of the matter in many astrophysical objects
- Magnetic field can be amplified by the gas contraction or shear motion.
- Even when the magnetic field is weak initially, the magnetic field grows in the short time scale and influences gas dynamics of the system

Astrophysical Jets

M87

- *Astrophysical jets: outflow of highly collimated plasma*
 - Microquasars, Active Galactic Nuclei, Gamma-Ray Bursts, Jet velocity $\sim c$.
 - Generic systems: Compact object
 \square White Dwarf, Neutron Star, Black Hole \square + Accretion Disk
- *Key Problem of Astrophysical Jets*
 - Acceleration mechanism
 - Collimation
 - Long term stability
- *Modeling of Astrophysical Jets*
 - Magnetohydrodynamics + Relativity
 - MHD centrifugal acceleration
 - Extraction of rotational energy from rotating black hole



Numerical Approach to Relativistic MHD

- RHD: reviews Marti & Muller (2003) and Fonts (2003)
- SRMHD: many authors
 - Application: Relativistic Riemann problems, Relativistic jet propagation, Pulsar wind nebule etc.
- GRMHD
 - **Fixed spacetime** (Yokosawa 1993; Koide, Shibata & Kudoh 1998; De Villiers & Hawley 2003; Gammie, McKinney & Toth 2003; Komissarov 2004; Anton et al. 2005; Annios, Fragile & Salmonson 2005)
 - Application: The structure of accretion flows onto black hole and/or formation of jets, BZ effect near rotating black hole, the formation of GRB jets in collapsars etc.
 - **Dynamical spacetime** (Duez et al. 2005; Shibata & Sekiguchi 2005; Anderson et al. 2006; Whisky MHD)

Propose to Make a New GRMHD Code

- The Koide's GRMHD Code (Koide, Shibata & Kudoh 1999; Koide 2003) has been applied to many high-energy astrophysical phenomena and showed pioneering results.
- However, the code can not perform calculation in highly relativistic ($\gamma > 5$) or highly magnetized regimes.
- The critical problem of the Koide's GRMHD code is the schemes can not guarantee to maintain divergence free magnetic field.
- In order to improve these numerical difficulties, we have developed a new 3D GRMHD code **RAISHIN** (**R**el**A**t**I**vi**S**tic magneto**H**ydrodynamc **s**Imulation**N**, RAISHIN is the Japanese ancient god of lightning).

4D General Relativistic MHD Equation

- General relativistic equation of conservation laws and Maxwell equations: □ □ □

$$\square\square\square\square\square\square\square\square_{\nu}(\rho U^{\nu}) = 0 \square\square\square \quad (\text{conservation law of particle-number})$$

$$\square\square\square\square\square\square\square\square_{\nu}T^{\mu\nu} = 0 \quad (\text{conservation law of energy-momentum})$$

$$\square\square\square\square\square\square\square\square_{\mu}F_{\nu\lambda} + \partial_{\nu}F_{\lambda\mu} + \partial_{\lambda}F_{\mu\nu} = 0 \quad (\text{Maxwell equations})$$

$$\square\square\square\square\square\square\square\square_{\mu}F^{\mu\nu} = -J^{\nu}$$

- Ideal MHD condition: $F_{\nu\mu}U^{\nu} = 0$
- metric □ □ $ds^2 = -\alpha^2 dt^2 + \gamma_{ij}(dx^i + \beta^i dt)(dx^j + \beta^j dt)$
- Equation of state : $p = (\Gamma - 1)u$

ρ : rest-mass density. p : proper gas pressure. u : internal energy. c : speed of light.

h : specific enthalpy, $h = 1 + u + p / \rho$.

Γ : specific heat ratio.

$U^{\mu\nu}$: velocity four vector. $J^{\mu\nu}$: current density four vector.

$\square^{\mu\nu}$: covariant derivative. $g_{\mu\nu}$: 4-metric. α : lapse function, β : shift vector, γ_{ij} : 3-metric

$T^{\mu\nu}$: energy momentum tensor, $T^{\mu\nu} = p g^{\mu\nu} + \rho h U^{\mu} U^{\nu} + F^{\mu\sigma} F^{\nu}_{\sigma} - g_{\mu\nu} F^{\lambda\kappa} F_{\lambda\kappa} / 4$.

$F_{\mu\nu}$: field-strength tensor,

Conservative Form of GRMHD

Equations (3+1 Form)

$$\frac{1}{\sqrt{-g}} \frac{\partial}{\partial t} (\sqrt{\gamma} D) + \frac{1}{\sqrt{-g}} \frac{\partial}{\partial x^i} (\sqrt{-g} D \tilde{v}^i) = 0, \quad \text{(Particle number conservation)}$$

$$\frac{1}{\sqrt{-g}} \frac{\partial}{\partial t} (\sqrt{\gamma} S_i) + \frac{1}{\sqrt{-g}} \frac{\partial}{\partial x^i} (\sqrt{-g} T_i^j) = T^{\mu\nu} \left(\frac{\partial g_{\nu i}}{\partial x^\mu} - \Gamma_{\nu\mu}^\sigma g_{\sigma i} \right) \quad \text{(Momentum conservation)}$$

$$\frac{1}{\sqrt{-g}} \frac{\partial}{\partial t} (\sqrt{\gamma} \tau) + \frac{1}{\sqrt{-g}} \frac{\partial}{\partial x^i} [\sqrt{-g} (\alpha T^{ti} - D \tilde{v}^i)] = \alpha \left(T^{\mu t} \frac{\partial \ln \alpha}{\partial x^\mu} - T^{\mu\nu} \Gamma_{\nu\mu}^t \right) \quad \text{(Energy conservation)}$$

$$\frac{1}{\sqrt{-g}} \frac{\partial}{\partial t} (\sqrt{\gamma} B^i) + \frac{1}{\sqrt{-g}} \frac{\partial}{\partial x^i} [\sqrt{-g} (\tilde{v}^j B^i - \tilde{v}^i B^j)] = 0. \quad \text{(Induction equation)}$$

\uparrow \uparrow \uparrow
 U (conserved variables) Fⁱ (numerical flux) S (source term)

\downarrow
 $D = \gamma \rho.$

$\sqrt{-g}$: determinant of metric

$$S_i = \alpha T_i^t = (\rho h + b^2) \gamma^2 v_i - \alpha b^0 b_i$$

$$\tau = \alpha^2 T^{tt} - D = (\rho h + b^2) \gamma^2 - (p + b^2/2) - \alpha^2 (b^t)^2 - D.$$

$$\tilde{v}^i = v^i - \beta/\alpha$$

Basics of Numerical RMHD Code

Nonconservative form (De Villier & Hawley (2003), Anninos et al.(2005))

$$\mathbf{B}(\mathbf{P})\frac{\partial \mathbf{P}}{\partial t} + \mathbf{C}(\mathbf{P})\frac{\partial \mathbf{P}}{\partial x} = 0$$

$\mathbf{U}=\mathbf{U}(\mathbf{P})$ - conserved variables,
 \mathbf{P} – primitive variables
 \mathbf{F} - numerical flux of \mathbf{U}

where

$$B_{km} = \frac{\partial U_{(k)}}{\partial P_{(m)}}, \quad C_{km} = \frac{\partial F_{(k)}}{\partial P_{(m)}},$$

Merit:

- they solve the internal energy equation rather than energy equation.
→ advantage in regions where the internal energy small compared to total energy (such as supersonic flow)
- Recover of primitive variables are fairly straightforward

Demerit:

- It can not applied high resolution shock-capturing method and artificial viscosity must be used for handling discontinuities

Basics of Numerical RMHD Code

Conservative form (Koide et al. (1999), Kommisarov (2001), Gammie et al (2003), Anton et al. (2004), Duez et al. (2005), Shibata & Sekiguchi (2005))

System of Conservation Equations

$$\frac{\partial \mathbf{U}}{\partial t} + \frac{\partial \mathbf{F}^i(\mathbf{U})}{\partial x^i} = \mathbf{S}(\mathbf{U})$$

$\mathbf{U}=\mathbf{U}(\mathbf{P})$ - conserved variables,

\mathbf{P} – primitive variables

\mathbf{F} - numerical flux of \mathbf{U} ,

\mathbf{S} - source of \mathbf{U}

Merit:

- High resolution shock-capturing method can be applied to GRMHD equations

Demerit:

- These schemes must recover primitive variables \mathbf{P} by numerically solving the system of equations after each step (because the schemes evolve conservative variables \mathbf{U})

Detailed Features of the Numerical Schemes

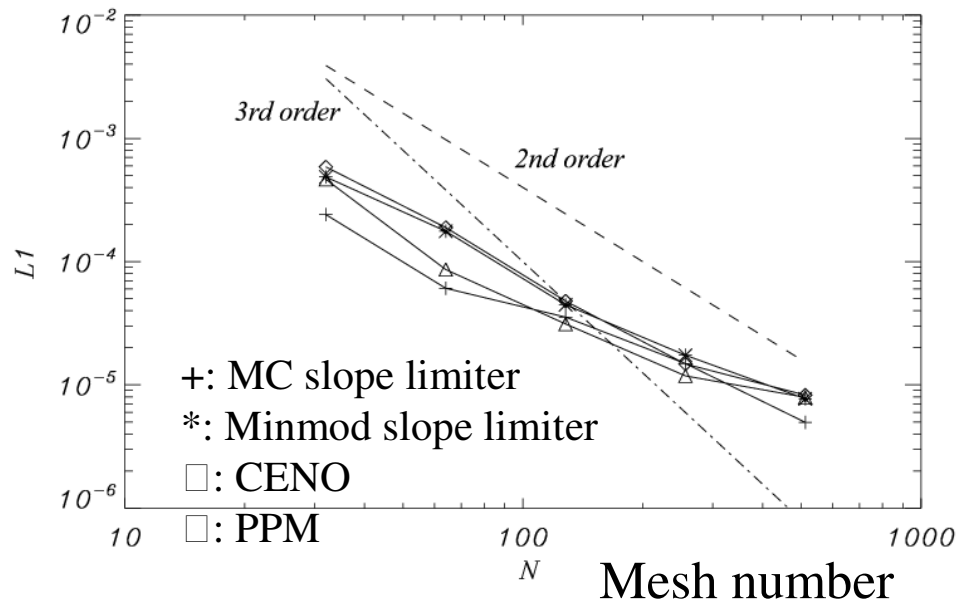
Mizuno et al. 2006a, astro-ph/0609004

- **RAISHIN** utilizes conservative, high-resolution shock capturing schemes to solve the 3D GRMHD equations (*metric is static*)
- * *Reconstruction*: PLM (Minmod & MC slope-limiter function), convex ENO, PPM
- * *Riemann solver*: HLL, HLLC approximate Riemann solver
- * *Constrained Transport*: Flux interpolated constrained transport scheme
- * *Time evolution*: Multi-step TVD Runge-Kutta method (second & third-order)
- * *Recovery step*: Koide 2 variable method and Noble 2D method

Ability of a New GRMHD code

- Multi-dimension (1D, 2D, 3D)
- Special and General relativity (static metric)
- Different coordinates (RMHD: Cartesian, Cylindrical, Spherical and GRMHD: Boyer-Lindquist of non-rotating or rotating BH)
- Different spatial reconstruction algorithms (4)
- Different approximate Riemann solver (2)
- Different time advance algorithms (2)
- Different recovery schemes (2)

Linear Alfven wave Propagation Tests



L1 norm of the error in density as a function of N (mesh number)

- Initially set linear Alfven mode and propagates periodic simulation box
- L1 norm equation

$$L_1(\delta\rho) = \int \left| \rho(t=0) - \rho\left(t = \frac{2\pi}{\omega}\right) \right| dx$$

i.e., the linear difference between the final state (after 1 cycle of simulation box) and the initial state

- All reconstruction schemes show the second-order of convergence

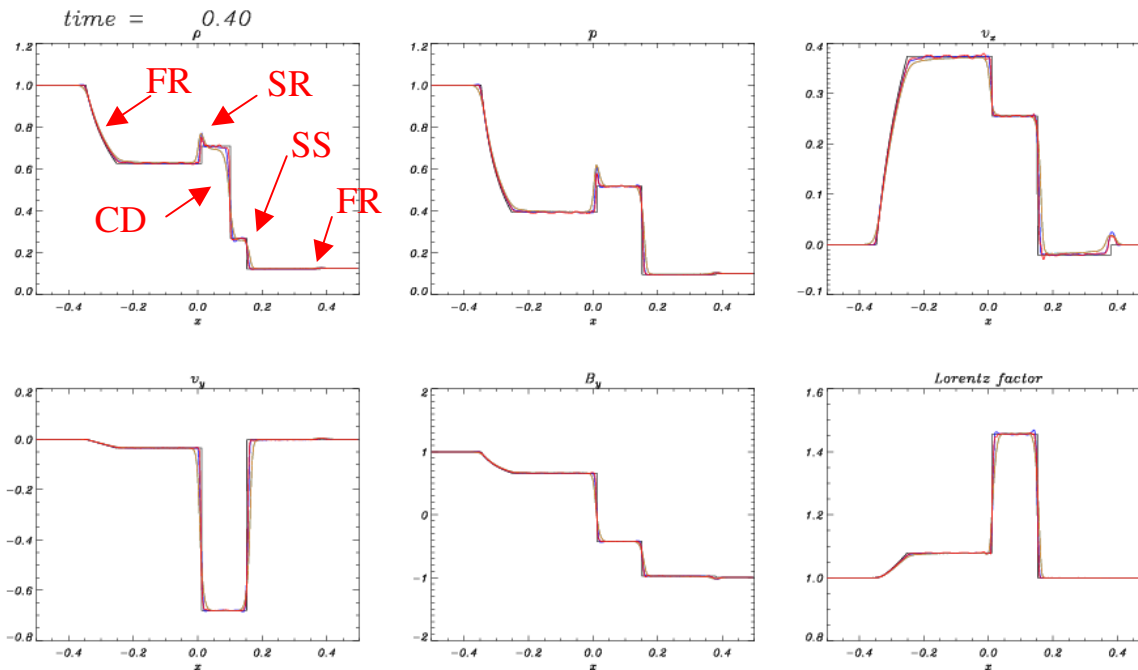
Relativistic MHD Shock-Tube Tests

Exact solution: Giacomazzo & Rezzolla (2006)

Test Type		ρ	p	v^x	v^y	v^z	B^x	B^y	B^z
Komissarov: Shock Tube Test1	$\Gamma = 4/3$								
	left state	1.0	1000.0	0.0	0.0	0.0	1.0	0.0	0.0
	right state	0.1	1.0	0.0	0.0	0.0	1.0	0.0	0.0
Komissarov: Collision Test	$\Gamma = 4/3$								
	left state	1.0	1.0	$5/\sqrt{26}$	0.0	0.0	10.0	10.0	0.0
	right state	1.0	1.0	$-5/\sqrt{26}$	0.0	0.0	10.0	-10.0	0.0
Barsara Test1 (Brio & Wo)	$\Gamma = 2$								
	left state	1.000	1.0	0.0	0.0	0.0	0.5	1.0	0.0
	right state	0.125	0.1	0.0	0.0	0.0	0.5	-1.0	0.0
Barsara Test2	$\Gamma = 5/3$								
	left state	1.0	30.0	0.0	0.0	0.0	5.0	6.0	6.0
	right state	1.0	1.0	0.0	0.0	0.0	5.0	0.7	0.7
Barsara Test3	$\Gamma = 5/3$								
	left state	1.0	1000.0	0.0	0.0	0.0	10.0	7.0	7.0
	right state	1.0	0.1	0.0	0.0	0.0	10.0	0.7	0.7
Barsara Test4	$\Gamma = 5/3$								
	left state	1.0	0.1	0.999	0.0	0.0	10.0	7.0	7.0
	right state	1.0	0.1	-0.999	0.0	0.0	10.0	-7.0	-7.0
Barsara Test5	$\Gamma = 5/3$								
	left state	1.08	0.95	0.40	0.3	0.2	2.0	0.3	0.3
	right state	1.00	1.0	-0.45	-0.2	0.2	2.0	-0.7	0.5
Generic Alfvén Test	$\Gamma = 5/3$								
	left state	1.0	5.0	0.0	0.3	0.4	1.0	6.0	2.0
	right state	0.9	5.3	0.0	0.0	0.0	1.0	5.0	2.0

Relativistic MHD Shock-Tube Tests

Balsara Test1 (Balsara 2001)





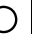









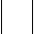
























































































Black: exact solution, Blue: MC-limiter, Light blue: minmod-limiter, Orange: CENO, red: PPM

400 mesh points

- The results show good agreement of the exact solution calculated by Giacomazzo & Rezzolla (2006).
- Minmod slope-limiter and CENO reconstructions are more diffusive than the MC slope-limiter and PPM reconstructions.
- Although MC slope limiter and PPM reconstructions can resolve the discontinuities sharply, some small oscillations are seen at the discontinuities.

Relativistic MHD Shock-Tube Tests

KO MC Min CENO PPM

- Komissarov: Shock Tube Test1            (large P)
- Komissarov: Collision Test           (large γ)
- Balsara Test1(Brio & Wu)          
- Balsara Test2                (large P & B)
- Balsara Test3                (large γ)
- Balsara Test4                (large P & B)
- Balsara Test5               
- Generic Alfven Test          

2D GRMHD Simulation of Jet Formation

Mizuno et al. 2006b, in preparation

Initial condition

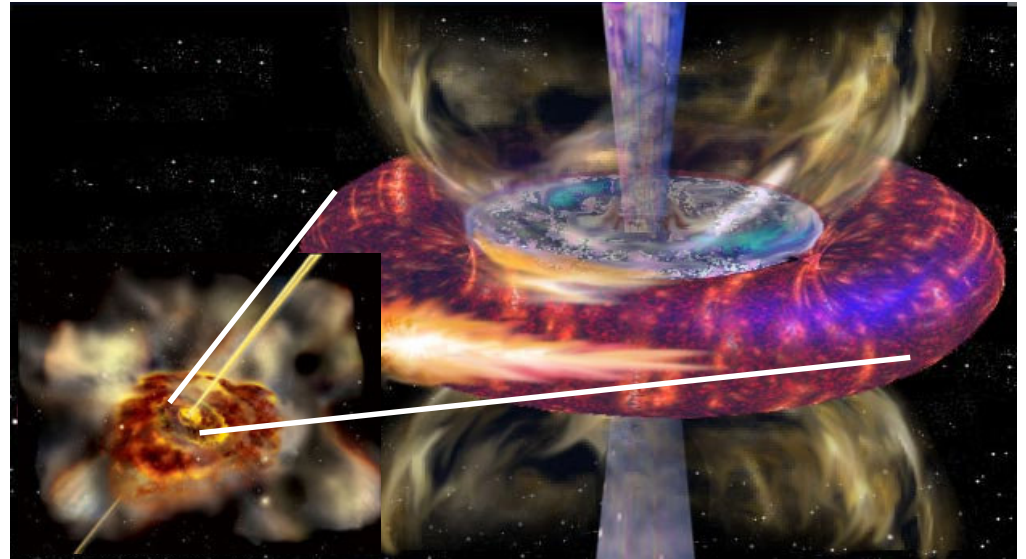
- Geometrically thin Keplerian disk ($\rho_d/\rho_c=100$) rotates around a black hole ($a=0.0, 0.95$)
- The back ground corona is free-falling to a black hole (Bondi solution)
- The global vertical magnetic field (Wald solution; $B_0=0.05(\rho c^2)^{1/2}$)

Numerical Region and Mesh points

- $1.1 \square 0.75) r_s < r < 40 r_s$, $0.03 < \theta < \pi/2$, with $128*128$ mesh points

Method

- minmod slope-limiter, HLL, flux-CT, RK3, Noble 2D method



Schematic picture of the jet formation near a black hole

Time evolution (Density)

non-rotating BH case ($B_0=0.05, a=0.0$)

Parameter

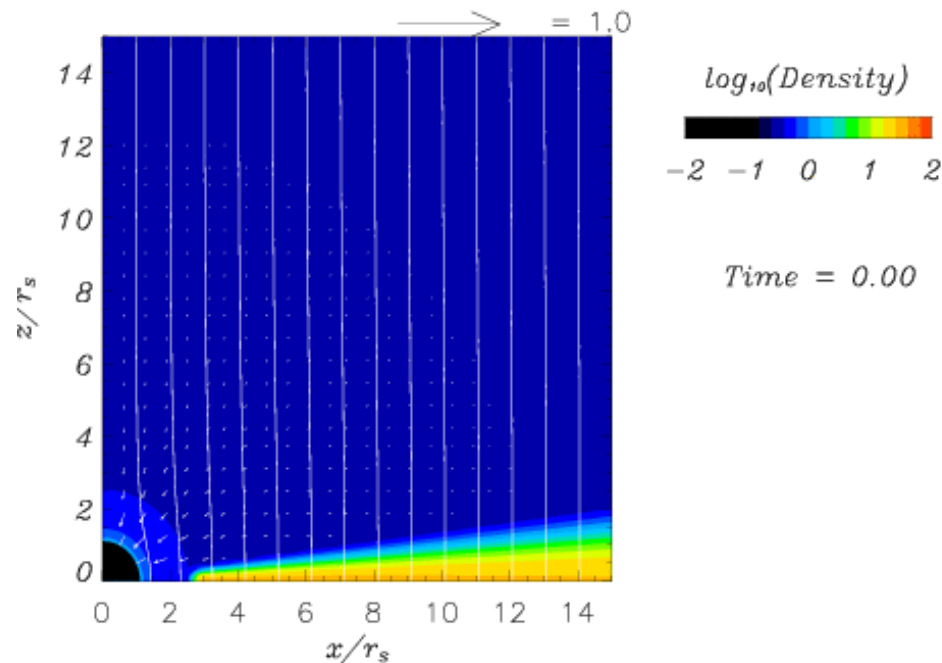
$B_0=0.05$

$a=0.0$

Color: density

White lines: magnetic
field lines

Arrows: poloidal
velocity



Time evolution (Density)

rotating BH case ($B_0=0.05, a=0.95$)

Parameter

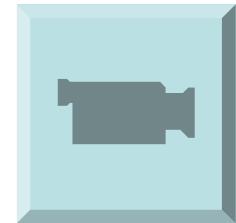
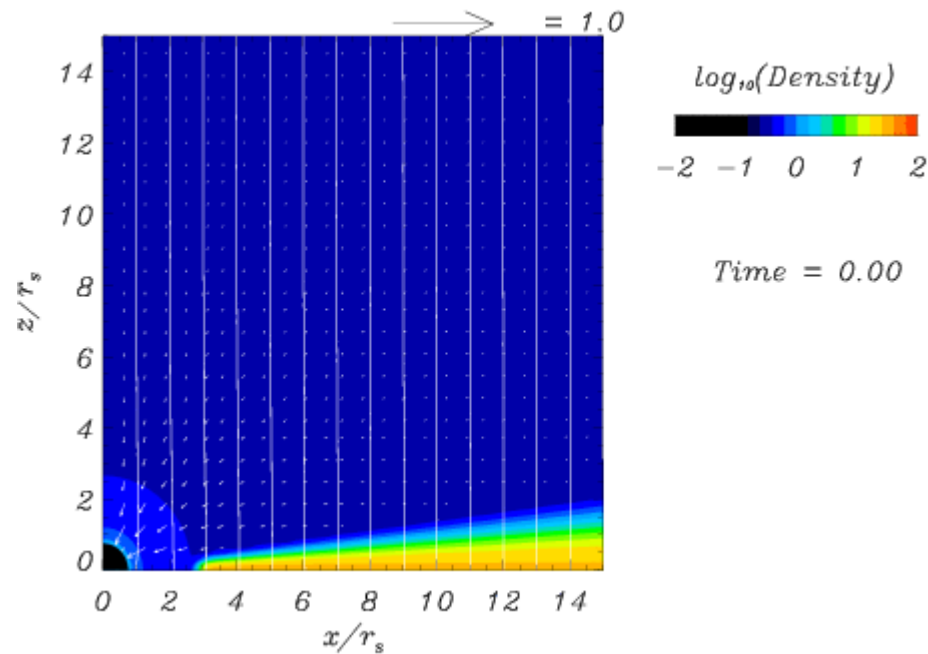
$$B_0=0.05$$

$$a=0.95$$

Color: density

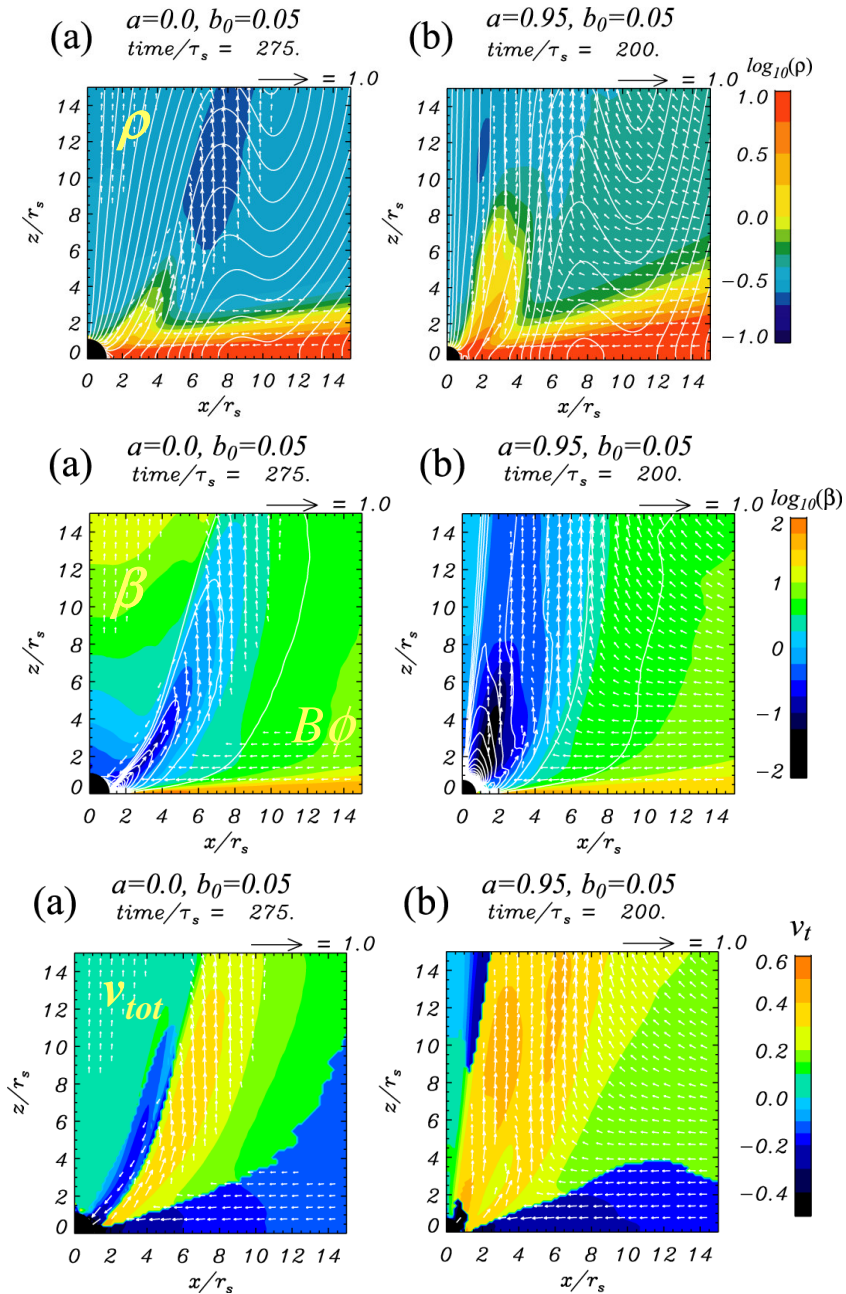
White lines: magnetic
field lines

Arrows: poloidal
velocity



Non-rotating BH Fast-rotating BH

Results



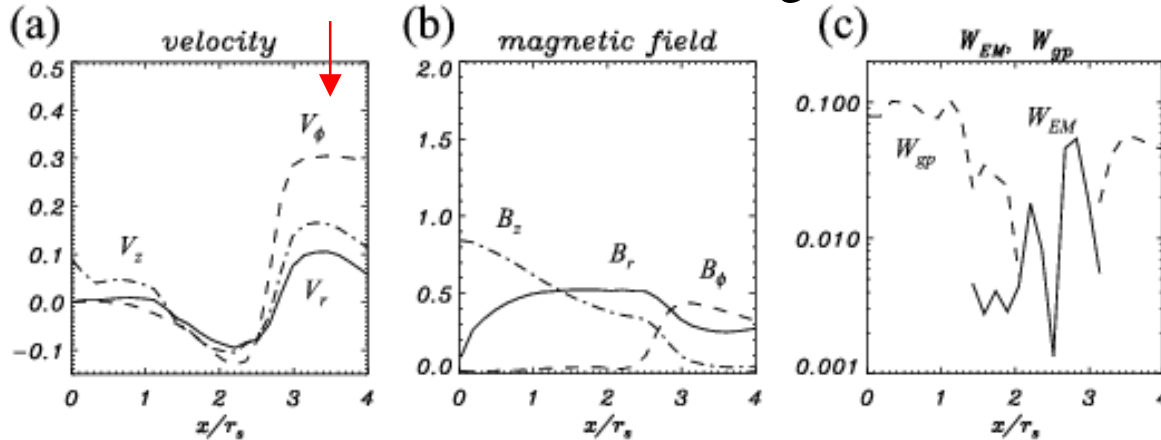
- The matter in the disk loses its angular momentum by magnetic field and falls to a black hole.
 - A centrifugal barrier decelerates the falling matter and make a shock around $r=2r_s$.
 - The matter near the shock region is accelerated by the $\mathbf{J} \times \mathbf{B}$ force and the gas pressure and forms jets.
 - These results are similar to previous work (Koide et al. 2000, Nishikawa et al. 2005).
- In the rotating black hole case, additional inner jets form by the magnetic field twisted resulting from frame-dragging effect.

White curves: magnetic field lines (density), toroidal magnetic field (plasma beta)
vector: poloidal velocity

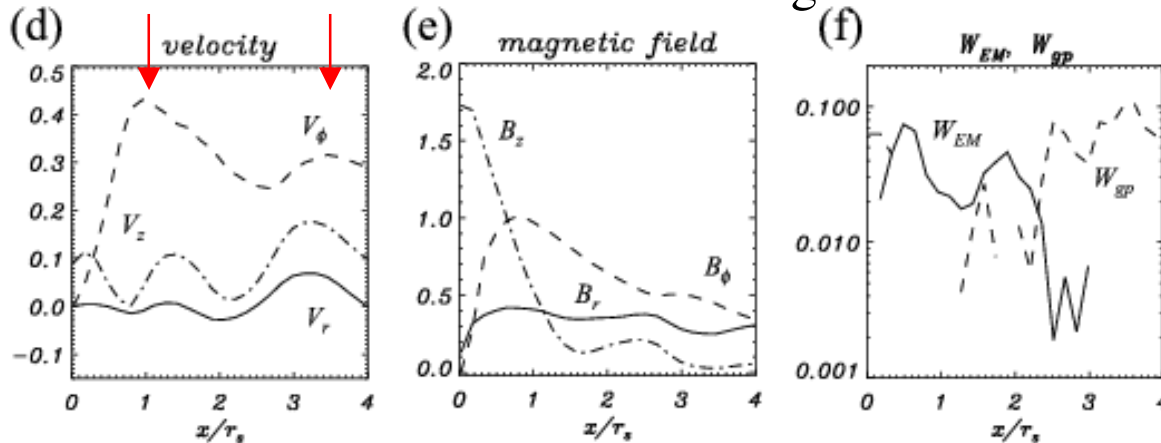
Results (Jet Properties)

W_{EM} : Lorentz force
 W_{gp} : gas pressure gradient

$a=0.0$ time/ $\tau_s = 270$. $z/r_s = 2$. Non-rotating BH



$a=0.95$ time/ $\tau_s = 195$. $z/r_s = 2$. Fast-rotating BH

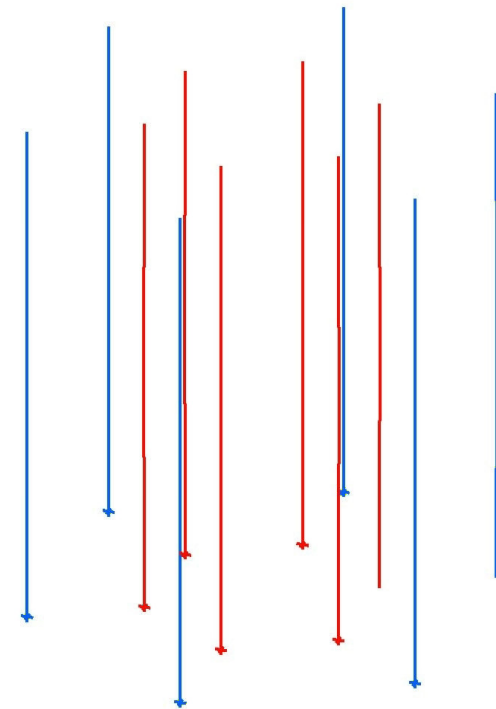


- **Outer jet**: toroidal velocity is dominant. The magnetic field is twisted by rotation of Keplerian disk. It is accelerated mainly by the gas pressure gradient (inner part of it may be accelerated by the Lorentz force).
- **Inner jet**: toroidal velocity is dominant (larger than outer jet). The magnetic field is twisted by the frame-dragging effect. It is accelerated mainly by the Lorentz force

Results (Magnetic Field properties)

3D GRMHD Simulation of Jet Formation

- 3D GRMHD Simulations of jet formation from rotating black hole with thin Keplerian disk (Nishikawa et al. 2006)
- Outer part of magnetic field is twisted by disk rotation
- Inner part of magnetic field is strongly twisted by the frame dragging effect
- Twisted magnetic field propagates outward as Alfvén wave.



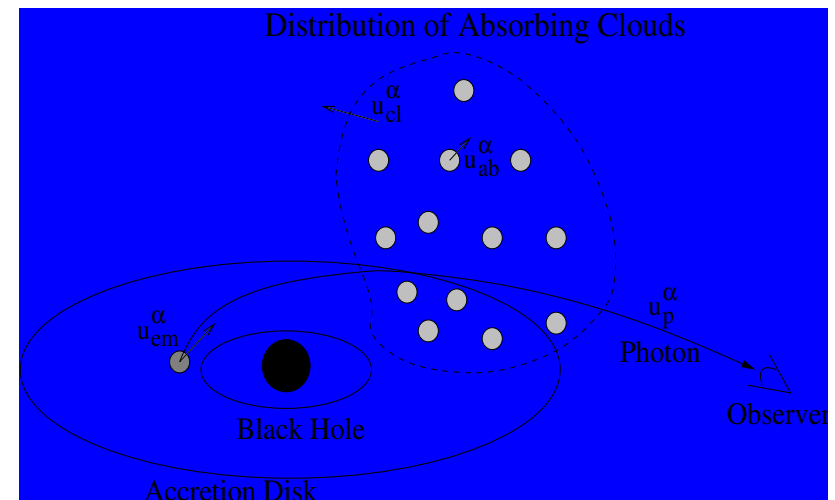
Time evolution of magnetic field line
at 6 rS and 12 rS

Relativistic Radiation Transfer

Collaborative works with S.Fuerst and K. Wu

- We have calculated the **Bremsstrahlung** and **Synchrotron radiation** from a disk-outflow system based on the results of our 2D GRMHD simulations (rotating BH cases).
- We consider a **covariant radiation transfer formulation** (Fuerst & Wu 2004, A&A, 424, 733) and solve the transfer equation using a ray-tracing algorithm.
- In this algorithm, we treat **general relativistic effect** (light bending, gravitational lensing, gravitational redshift, frame-dragging effect etc.).

Image of Emission, absorption & scattering

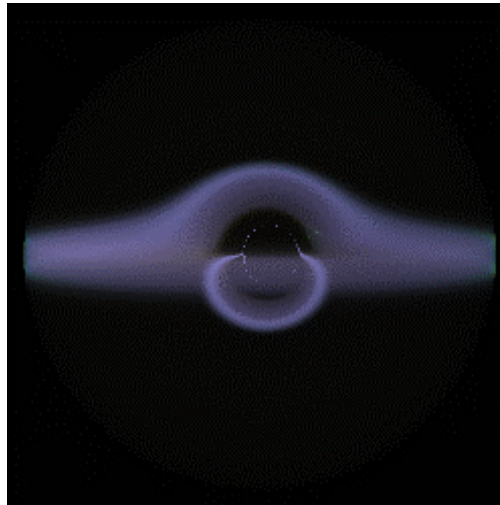


Relativistic Radiation Transfer

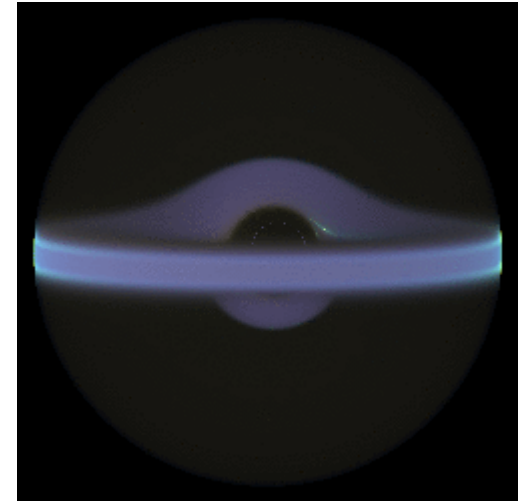
Fuerst, Mizuno, Nishikawa, 2006, in preparation

- The radiation image shows the front side of the accretion disk and the other side of the disk at the top and bottom regions.
- It is because the general relativistic effects.
- We can see the formation of two-component jet based on synchrotron radiation and the strong thermal radiation from hot dense gas near the BHs.
- A green-spark is a wired synchrotron on the surface of the disk

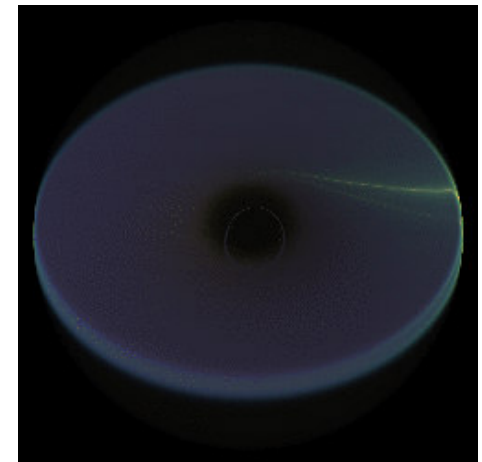
Radiation image seen from $\theta=85$ (optically thin)



Radiation image seen from $\theta=85$ (optically thick)



Radiation image seen from $\theta=45$ (optically thick)

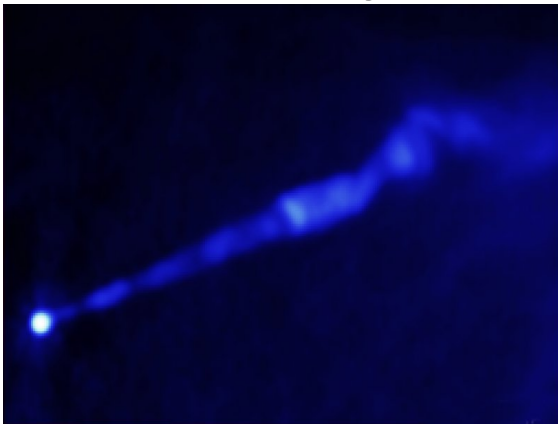


Stability Properties of Magnetized Spine-Sheath Relativistic Jets

Mizuno, Hardee & Nishikawa 2006c, in preparation

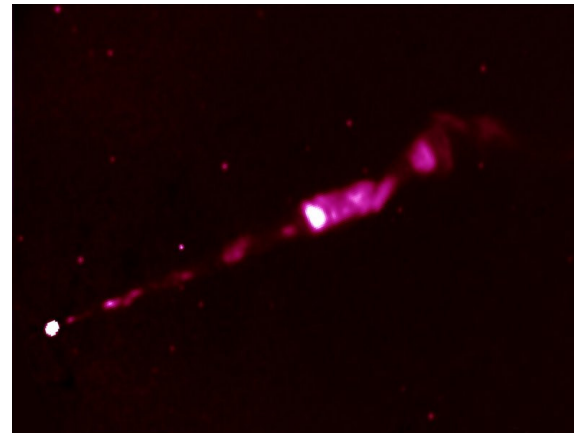
M87 Jet: Spine-Sheath Configuration?

VLA Radio Image (Biretta, Zhou, & Owen 1995)



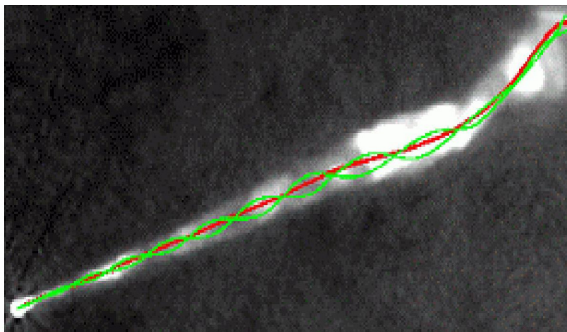
Typical Proper
Motions $< c$
Jet Sheath ?

HST Optical Image (Biretta, Sparks, & Macchetto 1999)



Typical Proper
Motions $> c$
Optical \sim inside
radio emission
Jet Spine ?

Jet Structures (Lobanov, Hardee, & Eilek 2003)



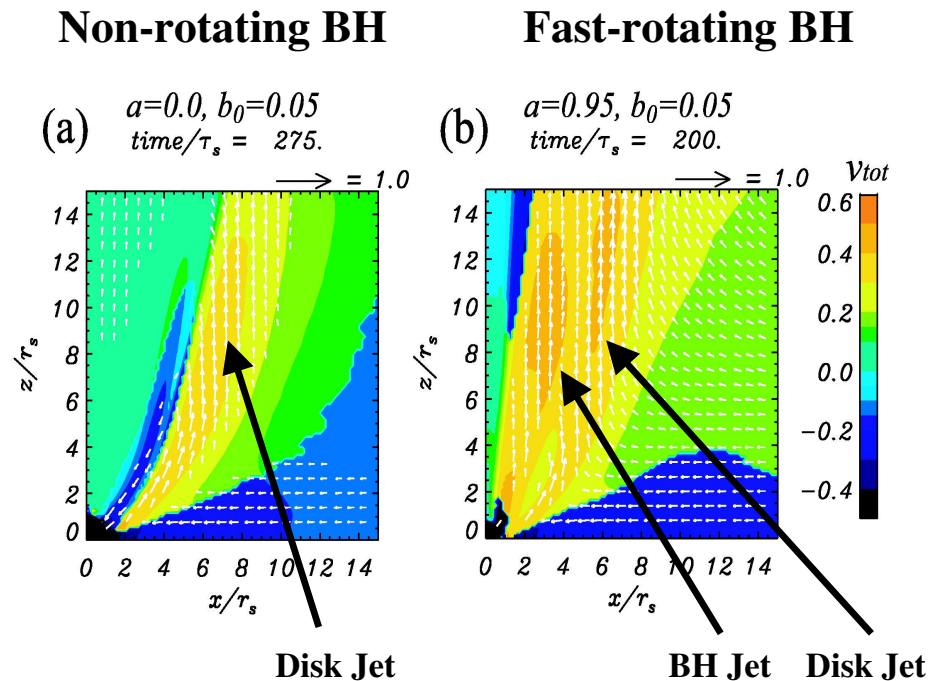
Optical & Radio twisted
filaments (green lines) &
helical twist (red line)
Spine-Sheath interaction ?

Key Questions of Jet Stability

- How do jets remain sufficiently stable when the jet propagates outward
- What are the Effects & Structure of current driven (CD)/Kelvin-Helmholtz (KH) Instability?
- Can CD/KH Structures be linked to Jet Properties?

Stability Properties of Magnetized Spine-Sheath Relativistic Jets

- GRMHD simulation results suggest that a jet spine driven by the magnetic fields threading the ergosphere may be surrounded by a broad jet sheath driven by the magnetic fields anchored in the accretion disk.
- This configuration might additionally be surrounded by a less highly collimated accretion disk wind from the hot corona.
- The jet speed is related to the Alfvén wave speed in the acceleration and collimation region implying Alfvén wave speeds near to light speed.



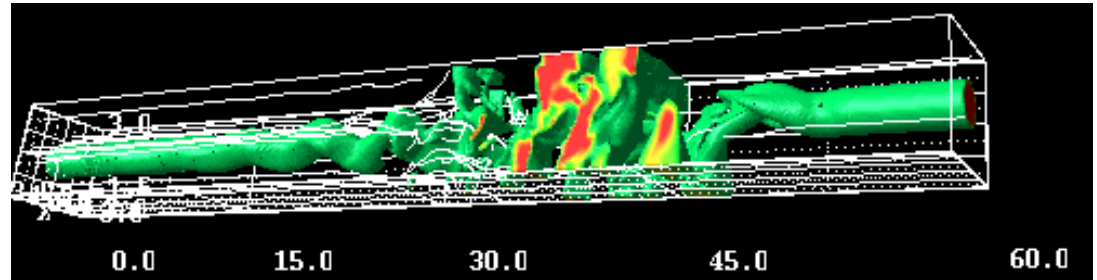
Total velocity distribution of 2D GRMHD Simulation of jet formation

3D Simulations of Spine-Sheath Jet Stability

Initial conditions for 3D RMHD simulations

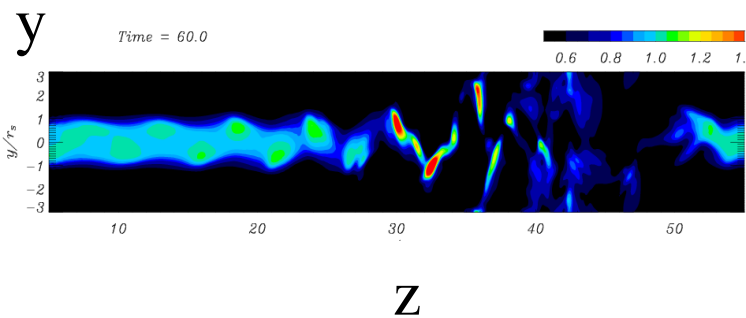
- Cylindrical Jet established across the computational domain
- $u_{jet} = 0.916 c$ ($\gamma_j=2.5$),
 $\rho_{jet} = 2 \rho_{ext}$
- External flow outside the jet,
 $u_{ext} = 0, 0.5c$
- Jet precessed to break the symmetry ($\omega_2=0.93$)
- **RHD**: $a_{jet} = 0.511 c$, $a_{ext} = 0.574 c$,
 $v_{A(j,e)} < 0.07 c$, *weakly magnetized*
- **RMHD**: $v_{Aj} = 0.45 c$, $v_{Ae} = 0.56 c$,
 $a_j = 0.23 c$, $a_e = 0.30 c$, *strongly magnetized*
- Cartesian coordinate (60*60*600 computational zone, $1r_j=10$)

Helically Twisted Density & Magnetic Structure

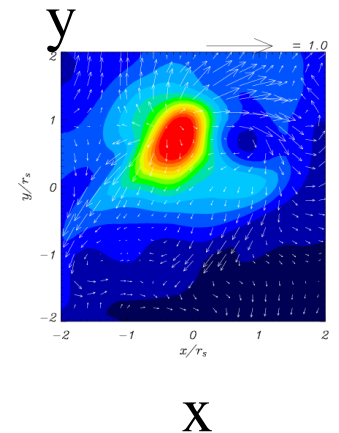


3D isovolume of density with B-field lines

Longitudinal cross section

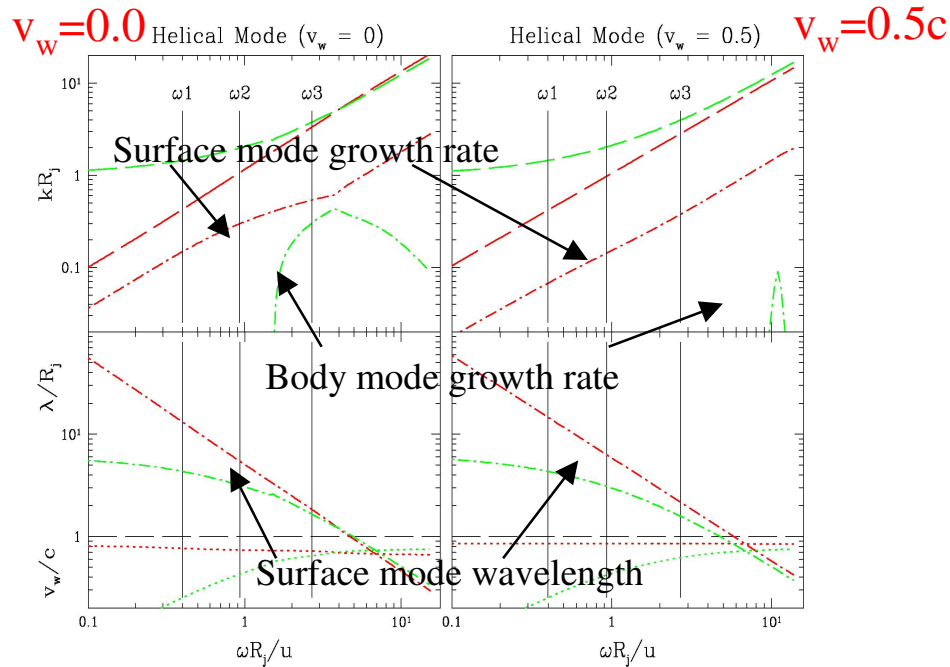


Transverse cross section



3D RHD Sheathed Jet Simulation & Theory

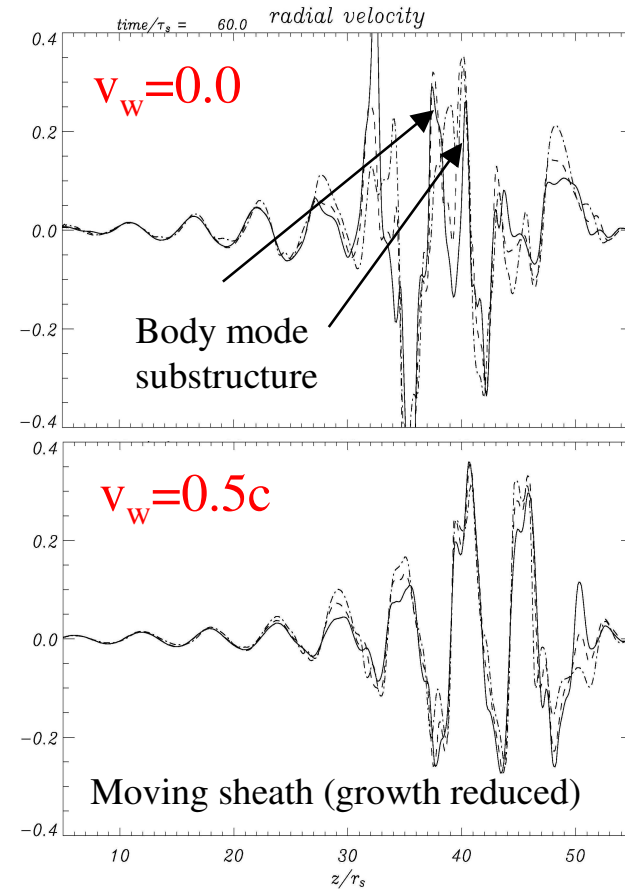
RHD Jet Dispersion Relation Solutions (Theory)



- A sheath with $v_w = 0.5c$ significantly reduces the growth rate (red dash-dot) of the surface mode at simulation frequency ω_2 , and slightly increases the wavelength.
- Growth associated with the 1st helical body mode (green dash-dot) is almost eliminated by sheath flow.

3D RHD Jet Simulation Results at ω_2

1D cut of radial velocity along jet

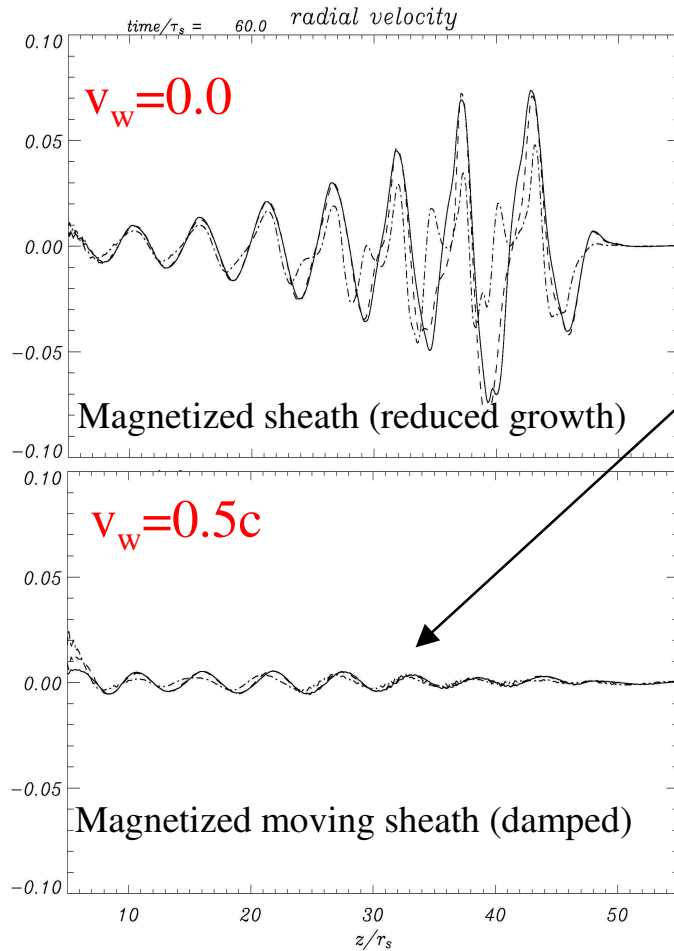


- The moving sheath reduces the growth rate and slightly increases the wave speed and wavelength as predicted.
- Substructure associated with the 1st helical body mode is eliminated by sheath flow as predicted.

3D RMHD Sheathed Jet Simulation & Theory

3D RMHD Jet Simulation Results at $\omega 2$

1D cut of radial velocity along jet



Magnetized sheath flow has reduced the “velocity shear” to less than the “surface” Alfvén speed:

$$\gamma_j^2 \gamma_e^2 (u_j - u_e)^2 < V_{As}^2$$

Note that for comparable conditions in spine and sheath $V_{As} = 2 \gamma_A (B^2/4\pi W)^{1/2}$ and $(B^2/4\pi W)^{1/2}$ can be $\gg c$.

- Growth of the KH instability driven by jet spine-sheath interaction is reduced significantly by mildly relativistic sheath flow and can be stabilized by magnetized sheath flow for spine Lorentz factors, γ_j , considerably larger than the Alfvén wave speed Lorentz factor, γ_A .
- This result for axial magnetic field remains valid in the presence of an additional toroidal component.

The magnetized sheath reduces growth rate relative to the fluid case and the magnetized sheath flow damped growth.

Summary

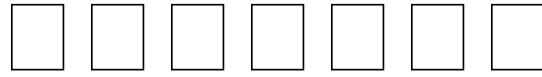
- We have developed a new three-dimensional general relativistic magnetohydrodynamic (GRMHD) code ``RAISHIN'' (RelAtivIStic magnetoHydrodynamic sImulationN, RAISHIN is the Japanese ancient god of lightning) by using a conservative, high-resolution shock-capturing scheme.
- The flux-interpolated, constrained transport scheme is used to maintain a divergence-free magnetic field.
- We have performed simulations of jet formation from a geometrically thin accretion disk near both non-rotating and rotating black holes. Similar to previous results (Koide et al. 2000, Nishikawa et al. 2005a) we find magnetically driven jets.
- It appears that the rotating black hole creates a second, faster, and more collimated inner outflow. Thus, kinematic jet structure could be a sensitive function of the black hole spin parameter.

Summary

- We have calculated the Bremsstrahlung and synchrotron radiations from a disk/outflow near a rotating black hole based on 2D GRMHD simulations using a covariant radiation transfer formulation.
- The calculation shows two-component jet based on synchrotron radiation and the ring-like thermal radiation from hot dense gas near the black hole.
- We have investigated stability properties of magnetized spine-sheath relativistic jets by the theoretical work and 3D RMHD simulations.
- The most important result is that destructive KH modes can be stabilized even when the jet Lorentz factor exceeds the Alfvén Lorentz factor. Even in the absence of stabilization, spatial growth of destructive KH modes can be reduced by the presence of magnetically sheath flow ($\sim 0.5c$) around a relativistic jet spine ($>0.9c$)

Future Work

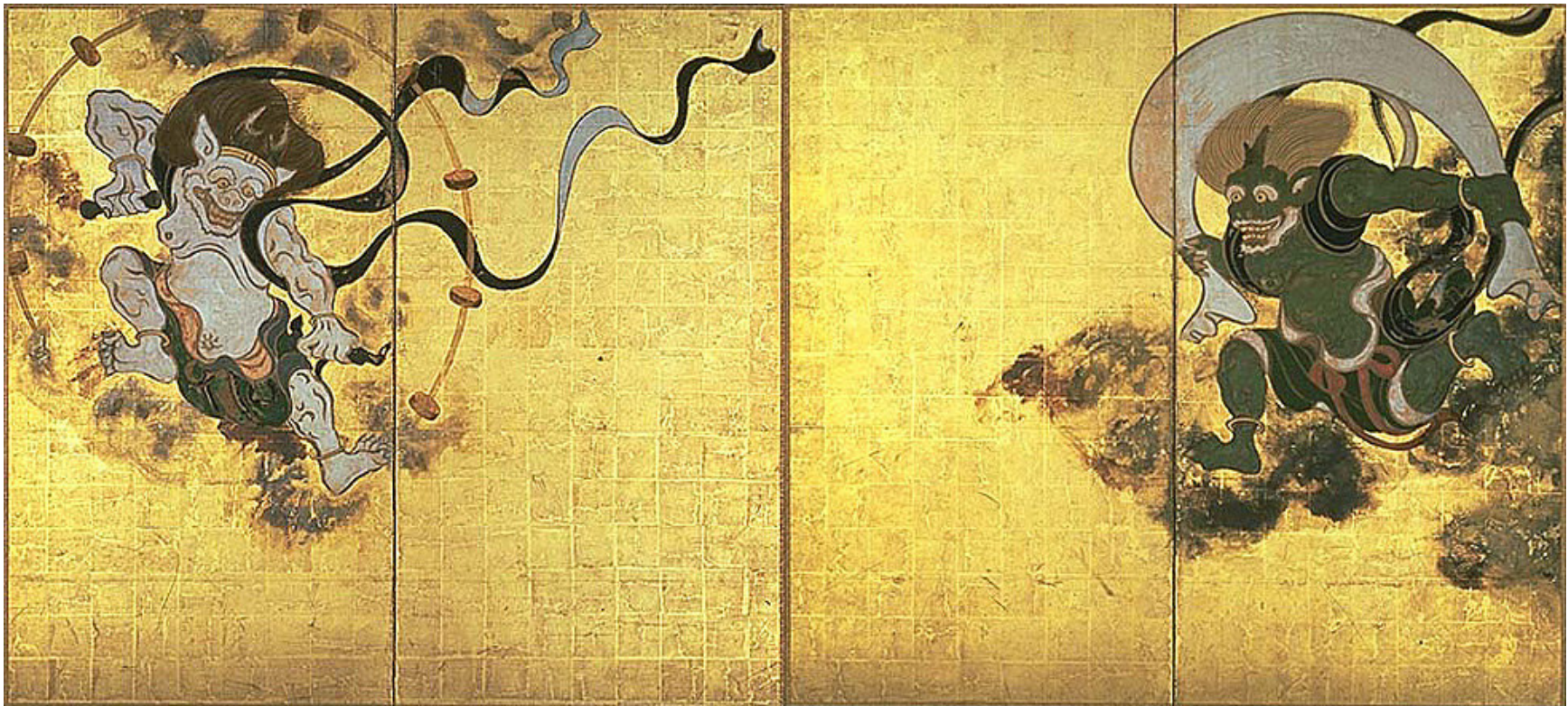
- Parallelization by using MPI
- Improve the EOS
- Include Neutrino (cooling, heating)
- Resistivity (extension to non-ideal MHD; e.g., Watanabe & Yokoyama 2006, ApJ, 647, L123)
- Include production of radiation and transfer (link to observation: Nishikawa et al. 2005, astro-ph/ 0509601)
- Include Nucleosynthesis post processing (e.g., Fujimoto et al. 2006, astro-ph/0602460)
- Couple with Einstein equation (dynamical spacetime)
- Apply to astrophysical phenomena in which relativistic outflows and/or GR essential (AGNs, microquasars, neutron stars, and GRBs etc.)



Wind God (Fushin) and Thunder God (Raishin) Screen

Raishin (Thunder God)

Fushin (Wind God)



By Ogata Korin (Edo era, 17 Century)
Tokyo National Museum